Environmental Science & Technology Letters

pubs.acs.org/journal/estlcu

Letter

Unprecedented Ambient Sulfur Trioxide (SO_3) Detection: Possible Formation Mechanism and Atmospheric Implications

Lei Yao, Xiaolong Fan, Chao Yan, Theo Kurtén, Kaspar R. Daellenbach, Chang Li, Yonghong Wang, Yishuo Guo, Lubna Dada, Matti P. Rissanen, Jing Cai, Yee Jun Tham, Qiaozhi Zha, Shaojun Zhang, Wei Du, Miao Yu, Feixue Zheng, Ying Zhou, Jenni Kontkanen, Tommy Chan, Jiali Shen, Joni T. Kujansuu, Juha Kangasluoma, Jingkun Jiang, Lin Wang, Douglas R. Worsnop, Tuukka Petäjä, Veli-Matti Kerminen, Yongchun Liu, Biwu Chu, Hong He,* Markku Kulmala,* and Federico Bianchi*

Cite This: *Environ. Sci. Technol. Lett.* 2020, 7, 809−818

Read Online

ACCESS | Metrics & More | Article Recommendations | Supporting Information

ABSTRACT: Sulfur trioxide (SO_3) is a crucial compound for atmospheric sulfuric acid (H_2SO_4) formation, acid rain formation, and other atmospheric physicochemical processes. During the daytime, SO_3 is mainly produced from the photo-oxidation of SO_2 by OH radicals. However, the sources of SO_3 during the early morning and night, when OH radicals are scarce, are not fully understood. We report results from two field measurements in urban Beijing during winter and summer 2019, using a nitrate-CI-APi-LTOF (chemical ionization-atmospheric pressure interface-long-time-of-flight) mass spectrometer to detect atmospheric SO_3 and H_2SO_4. Our results show the level of SO_3 was higher during the winter than during the summer, with high SO_3 levels observed especially during the early morning (~05:00 to ~08:30) and night (~18:00 to ~05:00 the next day). On the basis of analysis of SO_2, NO_x, black carbon, traffic flow, and atmospheric ions, we suggest SO_3 could be formed from the catalytic oxidation of SO_2 on the surface of traffic-related black carbon. This previously unidentified SO_3 source results in significant H_2SO_4 formation in the early morning and thus promotes sub-2.5 nm particle formation. These findings will help in understanding urban SO_3 and formulating policies to mitigate secondary particle formation in Chinese megacities.

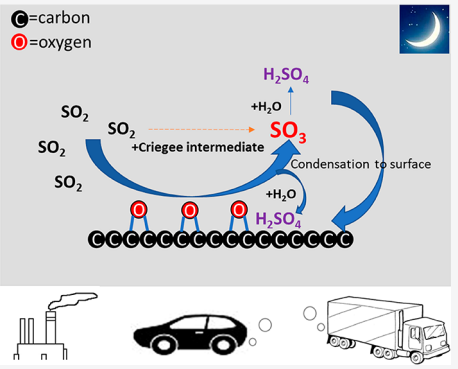

INTRODUCTION

Atmospheric SO_3 is a vital intermediate in gaseous H_2SO_4 formation, which in turn is a crucial compound in acid rain formation, new particle formation, secondary aerosol formation, and other atmospheric physicochemical processes.[1−8] During the daytime, when the intensity of UVB (ultraviolet radiation B) radiation that leads to the formation of OH radicals is high, SO_3 is mainly formed by atmospheric photo-oxidation of SO_2 by OH radicals. The mechanism of formation of SO_3 from photo-oxidation can be written as

$$SO_2 + OH + M \rightarrow HOSO_2 + M \quad (R1)$$

$$HOSO_2 + O_2 \rightarrow SO_3 + HO_2 \quad (R2)$$

However, during the early morning and at night, when OH radicals are scarce, the sources of atmospheric SO_3 remain unclear. Stabilized Criegee intermediates (sCI; general formula of R_1R_2COO) generated from the ozonolysis of alkenes have been found to be an important gas-phase oxidant for SO_2 in addition to OH (eq R3):[9,10]

$$R_1R_2COO + SO_2 \rightarrow R_1R_2C{=}O + SO_3 \quad (R3)$$

Besides gas-phase oxidation of SO_2 by OH radicals and sCI, SO_3 may also be formed from the heterogeneous oxidation of SO_2 on oxygen-functionalized graphene and soot surfaces.[11−13] He et al. have proposed that SO_2 molecules can react with surface epoxide groups of carbonaceous (or soot) aerosols, leading to SO_3 formation. These surface epoxy groups are considerably enhanced by atmospheric aging of soot particles in the presence of O_2.[12,14] Additionally, a recent theoretical study revealed high atmospheric water content could promote the oxidation of SO_2 to SO_3 by O_2 on carbonaceous aerosol surfaces.[15] Although extensive laboratory studies have reported that persistent particulate H_2SO_4 and sulfate can be formed from catalytic heterogeneous reaction between SO_2 and carbon (soot) particles in the presence of O_2, O_3, NO_x, NH_3, and water,[16−19] the

Received: August 7, 2020
Revised: September 24, 2020
Accepted: September 25, 2020
Published: September 25, 2020

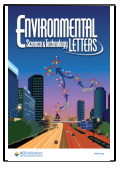

https://dx.doi.org/10.1021/acs.estlett.0c00615
Environ. Sci. Technol. Lett. 2020, 7, 809−818

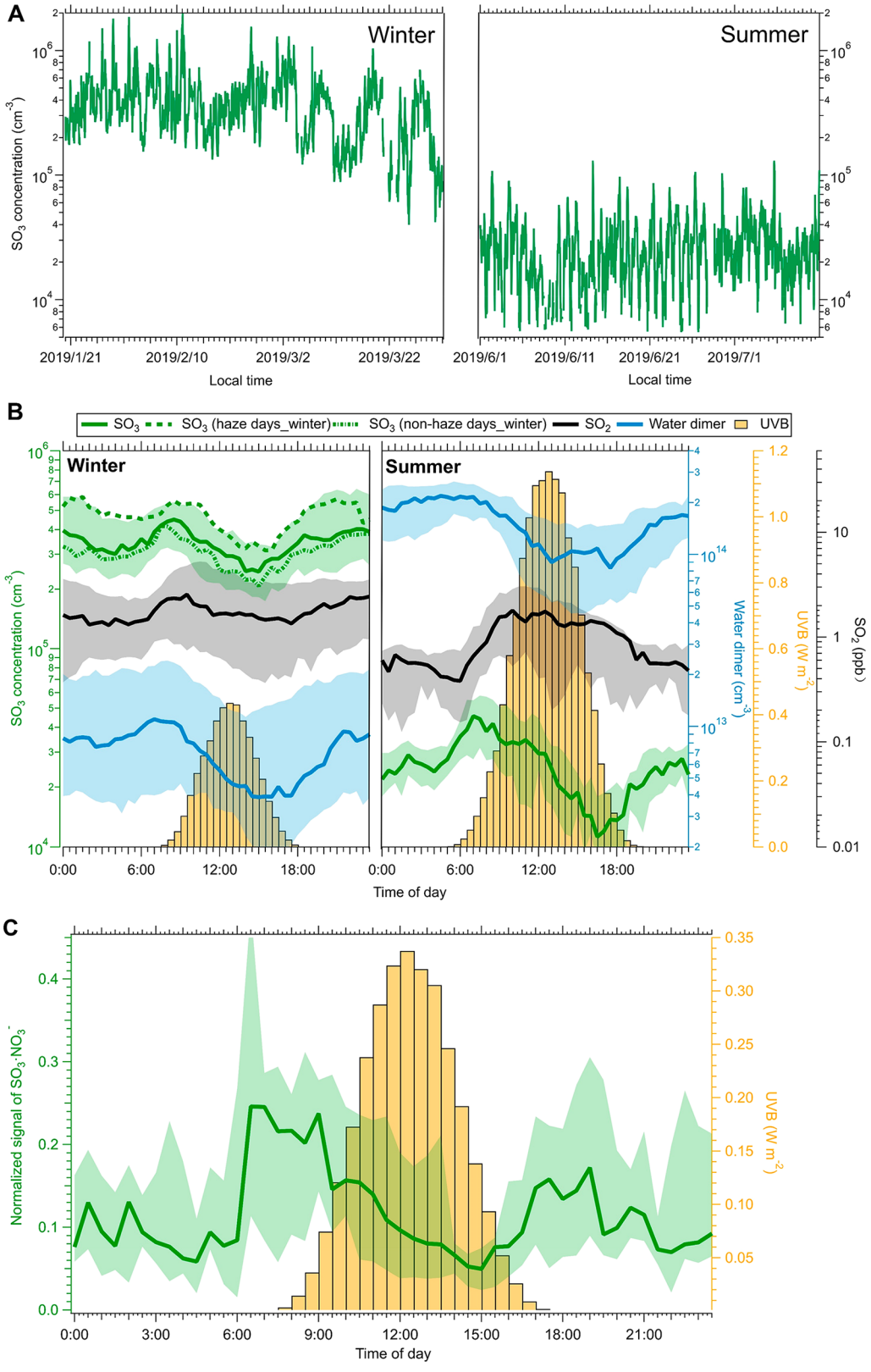

Figure 1. (A) Time series of SO_3 during the winter (January 20 to March 31, 2019) and summer (June 1 to July 10, 2019), (B) median diurnal patterns of SO_3, UVB, and atmospheric water dimer concentrations during the winter and summer, and (C) median normalized intensities of the atmospheric ion $SO_3{\cdot}NO_3^-$. Rainy and snowy days were excluded. The shadows show the values from the 25th to 75th percentile. In panel B, the dashed lines show diurnal variations of SO_3 during haze and nonhaze days. The water dimer concentration was calculated on the basis of temperature and relative humidity.[26,39] In panel C, the signals of atmospheric ion $SO_3{\cdot}NO_3^-$ were normalized by the sum of NO_3^- and $HNO_3{\cdot}NO_3^-$ that are dominant natural charged ions in urban Beijing (Figure S7).

https://dx.doi.org/10.1021/acs.estlett.0c00615
Environ. Sci. Technol. Lett. 2020, 7, 809−818

intermediate precursors of particulate sulfate, and the molecular-level details of this process, remain unclear. In addition to atmospheric formation of SO_3 via the oxidation of SO_2, a large amount of SO_3 can also be emitted to the air from coal-fired power plants and other industrial processes related to coal combustion and then be rapidly converted to H_2SO_4.[20−22]

In the atmosphere, the water-catalyzed hydration of SO_3 plays an essential role in H_2SO_4 formation (eq R4).

$$SO_3 + 2H_2O + M \rightarrow H_2SO_4 + H_2O + M \quad (R4)$$

In reaction R4, the second water molecule acts as a catalyst and significantly reduces the energy barrier of SO_3 hydration.[23,24] The rate coefficient of the reaction of SO_3 with the water dimer $[(H_2O)_2]$, or H_2O-catalyzed hydrolysis, is between 10^{-12} and 10^{-10} cm^3 $molecule^{-1}$ s^{-1}, resulting in a very short lifetime (<1 s) of SO_3.[23−26] In the atmosphere, besides water-catalyzed hydration, ammonia, sulfuric acid, formic acid, nitric acid, and oxalic acid (among others) can also act as catalysts for the SO_3 hydration process and thus facilitate H_2SO_4 formation.[25,27−29]

The detection of SO_3 is challenging owing to its high reactivity with water in ambient air. Various measurement technologies have been utilized for SO_3 detection in flue gases, including the controlled condensation method, absorption by isopropyl alcohol, selective reaction method with calcium oxalate, and spectroscopy and mass spectrometry methods.[22,30] The detection limits of these methods are unfortunately too high to measure trace-level SO_3 in ambient air. In some laboratory studies, the ions SiF_5^-, SF_6^-, $NO_3^-\cdot HNO_3$, and $n\text{-}C_3H_7NH_3^+$ have been used as reagent ions to detect SO_3.[31−35]

In this study, we deployed a nitrate-chemical ionization-atmospheric pressure interface-long-time-of-flight (nitrate-CI-APi-LTOF) mass spectrometer in two field measurements for atmospheric SO_3 and H_2SO_4 during the winter from January 20 to March 31 and during the summer from June 1 to July 10, 2019, in urban Beijing. This paper presents, for the first time, the trace-level measurement of gaseous SO_3 by a nitrate-CI-APi-LTOF mass spectrometer in an urban atmosphere. Additionally, atmospheric naturally charged ions were also measured from November 9 to 22, 2018. Combining the SO_3 measurements with data on trace gases, black carbon (BC), traffic flow, and atmospheric ions, we suggest a possible mechanism of formation of SO_3 in urban Beijing. We also probe the effects of SO_3 on atmospheric H_2SO_4 and sub-2.5 nm particle formation.

MATERIALS AND METHODS

Detection of SO_3 and H_2SO_4 by a Nitrate-CI-APi-LTOF Mass Spectrometer. The working principle of the nitrate-CI-APi-LTOF mass spectrometer is described in Text S2 and many other studies.[5,36] The high-resolution peak fit of $SO_3\cdot(NO_3^-)$ and its isotope peak $[^{34}SO_3\cdot(NO_3^-)]$ are depicted in Figure S1. The nitrate-CI-APi-LTOF mass spectrometer was calibrated by in situ-generated SO_3 and H_2SO_4[37] (Text S4). The calibration coefficients for SO_3 and H_2SO_4 are determined to be 1.7×10^{10} and 6.1×10^9 cm^{-3}, respectively (Figure S4). The ratio between the calibration coefficients of SO_3 and H_2SO_4 is 2.8, which is consistent with the theoretical prediction of a difference of a factor of 3 in the charging efficiency (Text S5). On the basis of repeat experiments, the 1σ of the SO_3 calibration coefficient was ±10%.

According to our quantum chemical calculation for the binding thermodynamics of $SO_3\cdot(NO_3^-)$ and $HNO_3\cdot(NO_3^-)$ ion−molecule clusters, the electronic binding energy of $SO_3\cdot(NO_3^-)$ is −44.4 kcal/mol, which is substantially higher than that of $HNO_3\cdot(NO_3^-)$ (−29.2 kcal/mol) (Texts S6 and S7 and Table S1). Thus, SO_3 molecules can be efficiently charged by nitrate ions. The highly favorable ligand exchange reaction between neutral SO_3 molecules and nitrate ions can be written as

$$SO_3 + NO_3^-\cdot(HNO_3) \rightarrow SO_3\cdot(NO_3^-) + HNO_3 \quad (R5)$$

Furthermore, on the basis of the quantum chemical calculation, reaction R6 is exothermal by 8.7 kcal/mol in free energy (Text S6). The lowest-free energy structure for $SO_3\cdot(NO_3^-)\cdot H_2O$ is depicted in Figure S6. Therefore, the hydrate complex intermediate ($SO_3\cdot H_2O$) also can be detected as $SO_3\cdot(NO_3^-)$.

$$SO_3\cdot H_2O + NO_3^-\cdot(HNO_3) \rightarrow SO_3\cdot(NO_3^-)\cdot H_2O + HNO_3 \quad (R6)$$

Besides the ligand exchange reaction, the reaction between SO_3 and NO_3^- can also lead to SO_4^- formation (eq R7).[32] However, SO_4^- can also be produced by the reaction of SO_2 with $O_2^-\cdot(H_2O)_n$.[34,38] From our ambient data, the averaged ratios of SO_4^- to $SO_3\cdot(NO_3^-)$ were 0.26 ± 0.07 (winter) and 2.51 ± 2.60 (summer). During the summer, a large abundance of $O_2^-\cdot(H_2O)_n$ favored SO_4^- formation. Hence, only the signal of $SO_3\cdot(NO_3^-)$ was taken into account in the SO_3 quantification, and it could cause a slight underestimation of SO_3 concentrations.

$$SO_3 + NO_3^- \rightarrow SO_4^- + NO_2 \quad (R7)$$

Atmospheric ions were also measured with the CI-APi-LTOF mass spectrometer by turning off the chemical ionization unit. Details of other auxiliary measuring instruments for trace gases, BC, meteorological parameters, and sub-3 nm particles can be found in Texts S8 and S9. Also, the calculation of condensation sink (CS) and quantification of SO_3 and H_2SO_4 were introduced in Texts S10 and S3.

RESULTS AND DISCUSSION

Abundance and Diurnal Behavior of SO_3 in the Winter and Summer. As shown in Figure 1A, the abundance of SO_3 was significantly higher in the winter than in the summer. During the winter, the mixing ratios of SO_3 varied from $\sim 4.0 \times 10^4$ to 1.9×10^6 molecules cm^{-3}. In comparison, during the summer, SO_3 concentrations ranged from $\sim 5.0 \times 10^3$ to 1.4×10^5 molecules cm^{-3}. Under 298 K and 1 atm, the atmospheric SO_3 concentration has been proposed to reach 10^5 molecules cm^{-3} around noon.[25] In this study, because the influence of ambient ions (i.e., $SO_3\cdot NO_3^-$) was not excluded and the hydrate complex intermediate ($SO_3\cdot H_2O$) also could be detected as $SO_3\cdot NO_3^-$ (eq R6), SO_3 concentrations could be overestimated. Median diurnal variations of SO_3 and SO_2 concentrations, water dimer concentrations $[(H_2O)_2$; computed from the relative humidity and temperature$]$,[26,39] and intensities of UVB (280−315 nm) on all measurement days during the winter and summer are illustrated in Figure 1B. The water dimer

https://dx.doi.org/10.1021/acs.estlett.0c00615
Environ. Sci. Technol. Lett. 2020, 7, 809−818

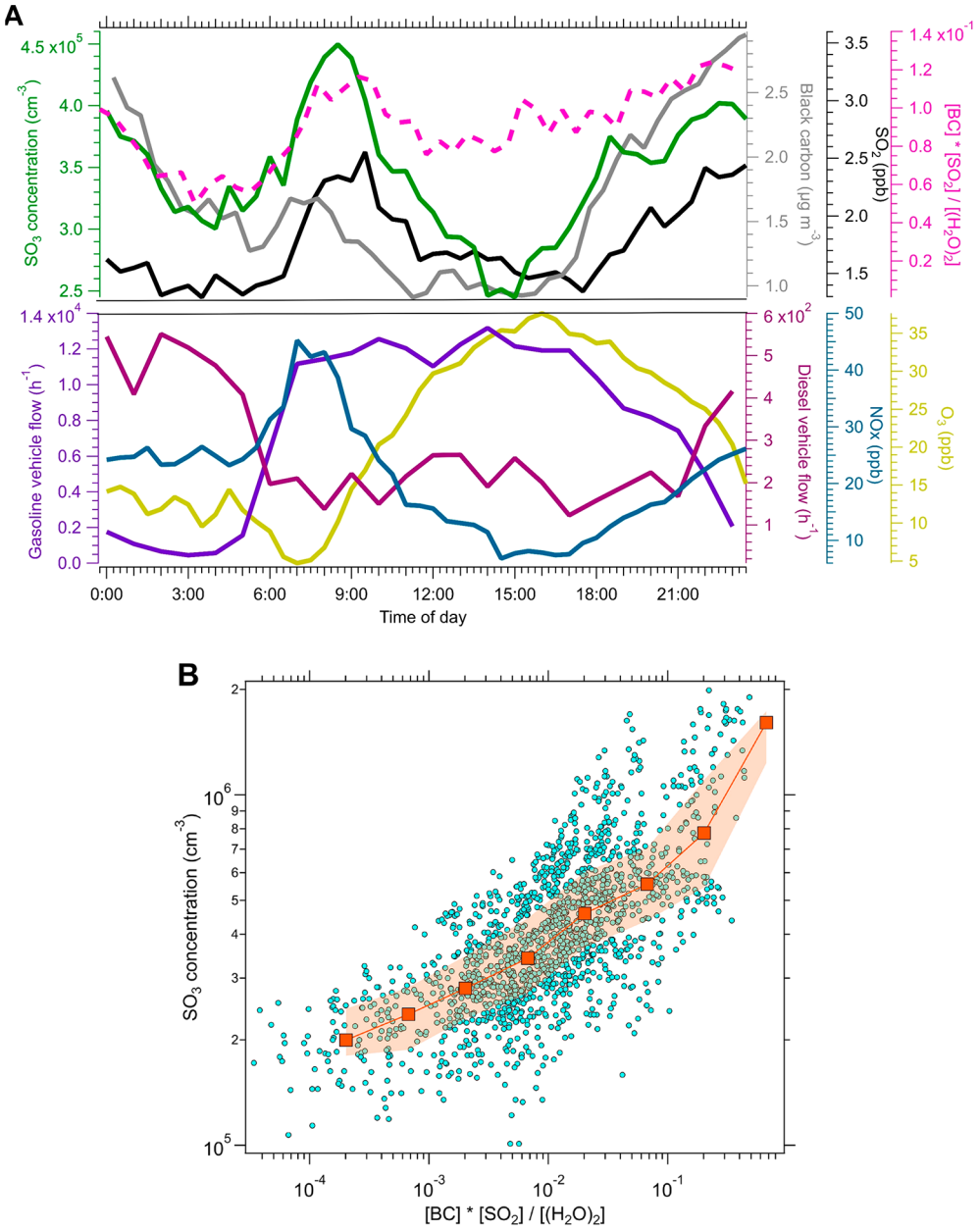

Figure 2. (A) Median diurnal variations in the concentrations of SO_3, SO_2, black carbon (BC), NO_x, the approximate abundance term $\{([BC][SO_2])/[(H_2O)_2]\}$ of SO_3, and gasoline and diesel vehicle flow of the "West Third Ring Road", which was ∼550 m to the west of the sampling station in 2017,[41] and (B) correlation between the SO_3 concentration and its approximate abundance term during the night and the early morning (from 18:00 to 08:00 the next day) for the whole field measurement during the winter. In panel A, the units of BC, SO_2, and water dimer $[(H_2O)_2]$ in approximate source terms were micrograms per cubic meter, molecules per cubic meter, and molecules per cubic meter, respectively. In panel B, the SO_3 concentrations were divided into logarithmic bins, and the median values in each bin are shown as squares. The orange shadow represents the values from the 25th to 75th percentile.

concentration during the summer was notably higher than during the winter. In contrast, the mixing ratio of SO_2 during the summer was lower than that during the winter. In the atmosphere, due to the large abundance of water, it is generally accepted that hydration to H_2SO_4 is the main fate of SO_3.[24] As a second water molecule is needed to lower the barrier of the SO_3 hydration reaction, the reaction rate effectively depends on the water dimer concentration.[23,40] Therefore, the low SO_3 concentrations during the summer likely result from the large abundance of the water dimer and low SO_2 concentration.

During the winter and summer, SO_3 showed similar diurnal patterns (Figure 1B). During the winter, SO_3 levels increased from ∼05:00 and reached their peak at ∼08:30. The abundance of SO_3 was higher during the early morning from ∼06:00 to ∼09:00 and night from ∼18:00 to ∼03:00 (the next day) than around noon. Similarly, during the summer, SO_3 concentrations increased from ∼4:00 and reached their peak values at ∼07:00. A peak of SO_3 in the early morning (∼04:00 to ∼08:00) was also observed. During both the winter and the summer, lower SO_3 concentrations were observed around noon when the water dimer concentration reached its minimum level (Figure 1B).

https://dx.doi.org/10.1021/acs.estlett.0c00615
Environ. Sci. Technol. Lett. 2020, 7, 809−818

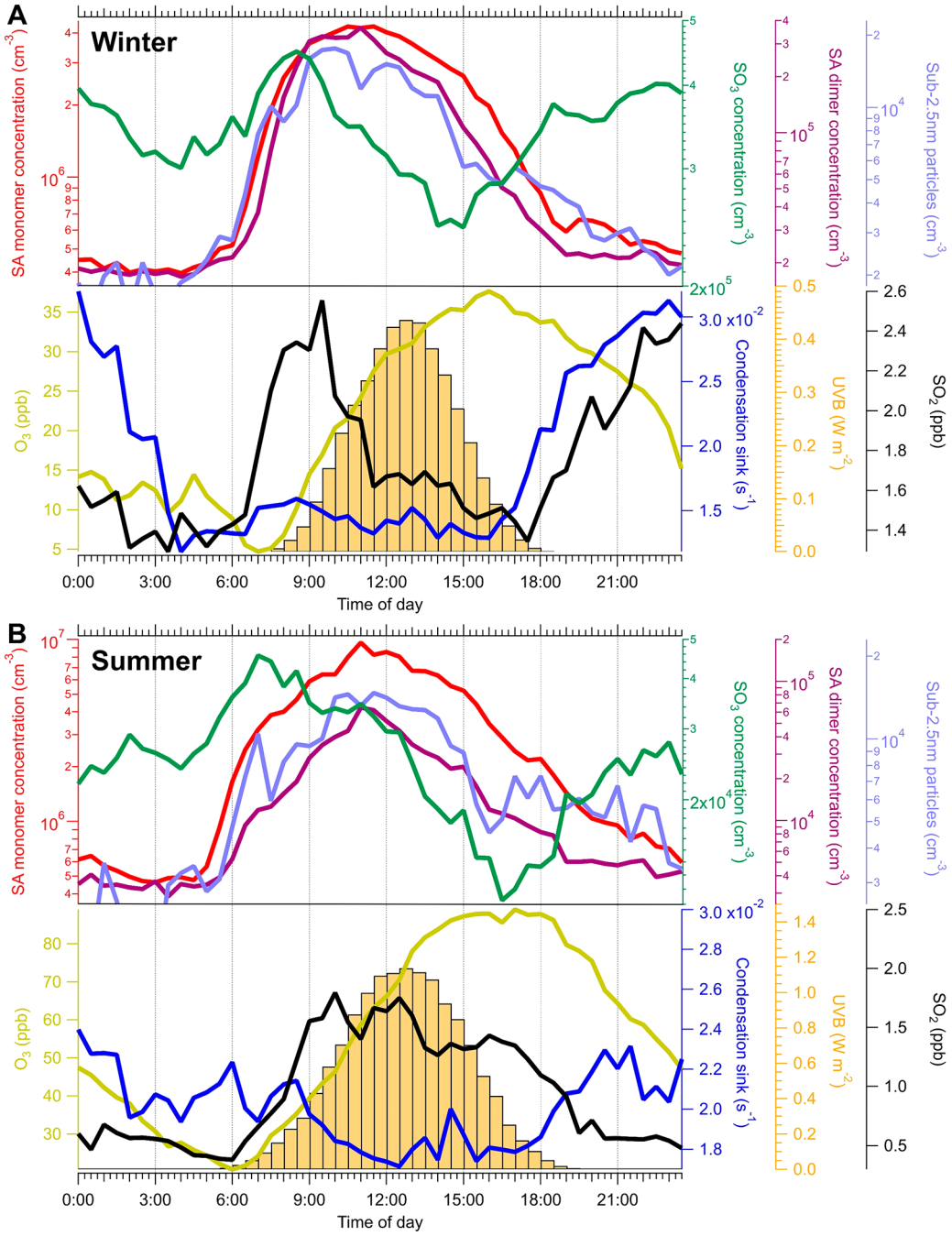

Figure 3. Median diurnal variations in the concentrations and intensities of SO_3, the sulfuric acid (SA) monomer (H_2SO_4) and dimer, sub-2.5 nm particles, SO_2, O_3, UVB, and condensation sink (CS) during the (A) winter and (B) summer.

Besides water-catalyzed hydration, around noon, a large abundance of other atmospheric components (e.g., H_2SO_4, HCOOH, HNO_3, and oxalic acid) also promoted the conversion of SO_3, leading to relatively short lifetimes. In addition, diel patterns of SO_3 on nonhaze and haze days in winter are also shown in Figure 1B. The abundance of SO_3 exhibited a similar daily pattern during both haze and nonhaze days (Text S8), though the actual values were higher on haze days.

The averaged mass spectra of atmospheric naturally charged ions for a day are shown in Figure S7. The dominant anions in urban Beijing are nitrate ions (NO_3^- and $HNO_3{\cdot}NO_3^-$), similar to the case in Shanghai.[5] Therefore, the normalized intensity of $SO_3{\cdot}NO_3^-$ by the sum of nitrate ions also can represent the abundance of SO_3 in the air. Figure 1C shows the diel variation of the normalized signals of $SO_3{\cdot}NO_3^-$ in November 2018. The normalized signals also exhibited two peaks, in the early morning (~6:00 to ~9:00) and at night (~17:00 to ~20:00).

Potential Source Identification for SO_3. To investigate the possible sources of SO_3 molecules during the early morning and night, we monitored other trace gases (SO_2 and NO_x), BC, and traffic flow of the main road nearby.[41] During the summer, the average SO_3 concentration was 2.9×10^4 molecules cm^{-3}, which is likely close to the detection limit of the instrument. Hence, the possible source identification for

https://dx.doi.org/10.1021/acs.estlett.0c00615
Environ. Sci. Technol. Lett. 2020, 7, 809−818

SO_3 was focused on winter data. During the winter, the median concentrations of SO_2, NO_x, and BC in $PM_{2.5}$ exhibited diurnal trends similar to those of SO_3 (Figure 2A). On the basis of previous studies of SO_2 and together with stable weather conditions (low wind speeds and shallow mixing layer) (Text S11 and Figure S8), the elevated SO_2 concentration during the early morning could mainly be attributed to local emissions (e.g., residential and industry emission) and transportation.[42−50] BC concentrations were tightly linked with traffic emission dominated by diesel vehicles (Figure 2A).

During the early morning, the UVB intensity was low, which meant that OH radical concentrations from photochemistry were also low, because of the linear correlation between OH concentrations and the ozone photolysis frequency [j(O1D)] in Beijing during daytime.[51] During a summer night in the suburban area of Beijing, OH radical concentrations from ∼0.5 to 3 × 10^6 cm^{-3} still can be observed.[52,53] Nevertheless, during the winter in suburban Beijing, the mean observed OH concentrations were <3 × 10^5 cm^{-3} at night and <1 × 10^6 cm^{-3} in the early morning (06:00−09:00).[54,55] Hence, the oxidation of SO_2 by OH radicals was not the main source for SO_3 during the early morning and night. In addition, during the early morning, the median ozone concentration was only ∼5 ppb, which was low in comparison to the values during the rest of the day, resulting in a minor contribution to SO_3 production from the reaction between sCI and SO_2. Although SO_3 molecules can also be co-emitted with SO_2,[20−22,56,57] transportation is not feasible for SO_3 owing to its short lifetime (<1s) in the air. Previous studies based on quantum chemical calculations have suggested that the heterogeneous reaction between SO_2 and soot can lead to SO_3 formation.[11,12] If this mechanism were to dominate SO_3 formation, and further assuming that the SO_3 is removed by reaction with the water dimer, the concentration of SO_3 would be proportional to ([BC]·[SO_2])/[$(H_2O)_2$]. Figure 2A shows that during the early morning (06:00−09:00) and night (from 18:00 to 6:00 the next day), the median diurnal variations of SO_3 and ([BC][SO_2])/[$(H_2O)_2$] were consistent with each other. Also, for the whole measurement period during the winter from 18:00 to 08:00 the next day, the correlation between SO_3 and this approximate abundance term was positive [r = 0.7; P < 0.0001 (Figure 2B)]. Furthermore, on nonhaze days, SO_3 was tightly linked to particulate sulfate, implying SO_3 may originate from heterogeneous reaction (Figure S9). Therefore, our results together suggested the heterogeneous reaction between SO_2 and BC could be the possible source of SO_3 during the early morning and at night. However, other formation mechanisms (e.g., Criegee intermediate and SO_2) may also contribute.[9]

Enhancement of Sulfuric Acid and Sub-2.5 nm Particle Formation. Median diurnal variations of the concentrations or intensities of H_2SO_4, the sulfuric acid dimer (H_2SO_4·HSO_4^-), SO_3, sub-2.5 nm particles, CS, SO_2, ozone, and UVB during the winter and summer are shown in panels A and B of Figure 3A and B, respectively. During the winter and summer, elevated levels of SO_3 and H_2SO_4 were simultaneously observed in the early morning. During the winter, the median concentrations of H_2SO_4 during the early morning were comparable with that around noon. In addition, it showed a good correlation (r = 0.7) between atmospheric ions of HSO_4^- and SO_3·NO_3^- during the early morning (5:00−8:00) and night (from 18:00 to 5:00 the following day) (Figure S10). Thus, the SO_3 formed from nonphotochemical processes enhanced H_2SO_4 formation during the early morning and night. In a recent study in urban Beijing, under clean conditions, oxidation of SO_2 by oxidants produced in the ozonolysis of alkenes (i.e., sCI and "dark" OH) was suggested as a source of H_2SO_4 during the night.[58] This study also pointed out that, under polluted conditions, additional sources of H_2SO_4 exist. Hence, during the night in urban Beijing, H_2SO_4 can be enhanced both by SO_3 molecules produced by the heterogeneous reaction between BC and SO_2 and by the oxidation of SO_2 by oxidants from ozonolysis of alkenes.

As shown in Figure 3, during the winter or summer, the median concentrations of H_2SO_4, H_2SO_4·HSO_4^-, and sub-2.5 nm particles followed the same diurnal behavior. The concentrations of H_2SO_4·HSO_4^- and sub-2.5 nm particles started to increase at ∼5:00. During the early morning during the winter, the median concentrations of H_2SO_4·HSO_4^- and sub-2.5 nm particles were comparable with that around noon. On the basis of the studies in urban Shanghai, if atmospheric bases were abundant, the sulfuric acid dimer could be treated as an indicator of nanocluster formation.[5,59] In urban Beijing, the concentrations of atmospheric bases (e.g., amines and ammonia) may also be sufficient for efficient clustering. Thus, the increased level of formation of SO_3, possibly produced by the oxidation of SO_2 on top of soot particles, can intensify the production of secondary particles and enhance gas to particle conversion during the early morning and night. We note that the contribution to nanoclusters of traffic, or the reaction of SO_3 with ammonia/methanol, cannot be wholly excluded.[25,60−62] Our results together point toward the need to control the emission of SO_2 and soot to mitigate secondary aerosol formation in urban Beijing.

■ ASSOCIATED CONTENT

Supporting Information

The Supporting Information is available free of charge at https://pubs.acs.org/doi/10.1021/acs.estlett.0c00615.

Description of the sampling site (Text S1), the nitrate-CI-APi-LTOF mass spectrometer (Text S2), detection of sulfuric acid with nitrate reagent ions (Text S3), detailed calibration experiment for SO_3 (Text S4), quantum chemical calculations (Text S6), computational details (Text S7), $PM_{2.5}$, black carbon, particulate sulfate, trace gases, meteorological parameters, and UVB measurements (Text S8), sub-3 nm particle measurements (Text S9), calculation of condensation sink (Text S10), source identification of SO_2 during the winter (Text S11), high-resolution peak fitting of the $^{32}SO_3$·NO_3^- peak and its $^{34}SO_3$·NO_3^- main isotope peak (Figure S1), schematic of the calibration experiment setup (Figure S2), time series of normalized signals of H_2SO_4 and SO_3, and [H_2O] in the calibration experiment (Figure S3), correlation between normalized SO_3 signals measured by the CI-APi-LTOF mass spectrometer and SO_3 concentrations formed by photo-oxidation of SO_2 by OH radicals (Figure S4), optimized structure of the SO_3·(NO_3^-) cluster (Figure S5), lowest-free energy (at 298 K) structure found for SO_3·(NO_3^-)·H_2O (Figure S6), averaged mass spectra of atmospheric naturally charged ions for one whole

https://dx.doi.org/10.1021/acs.estlett.0c00615
Environ. Sci. Technol. Lett. 2020, 7, 809−818

day (November 10, 2018) (Figure S7), median diurnal variation of the concentrations of SO_3 and SO_2, the mixing layer heights (MLH), intensities of UVB, and wind speeds during the winter (Figure S8), time profile of the SO_3 concentration and mass concentration of sulfate in $PM_{2.5}$ and median diel variation of SO_3 and sulfate for all nonhaze days during the winter measurement period (Figure S9), relationship between the atmospheric ion signals of HSO_4^- and $SO_3{\cdot}NO_3^-$ during the night (from 18:00 to 5:00 next day) and early morning (5:00−8:00) from November 9 to 22, 2018 (Figure S10), and comparison of the binding thermodynamics of $HNO_3{\cdot}(NO_3^-)$ and $SO_3{\cdot}(NO_3^-)$ ion−molecule clusters (Table S1) (PDF)

AUTHOR INFORMATION

Corresponding Authors

Federico Bianchi − *Aerosol and Haze Laboratory, Beijing Advanced Innovation Center for Soft Matter Science and Engineering, Beijing University of Chemical Technology, Beijing 100089, China; Institute for Atmospheric and Earth System Research/Physics, Faculty of Science, University of Helsinki, Helsinki 00560, Finland;* orcid.org/0000-0003-2996-3604; Email: federico.bianchi@helsinki.fi

Markku Kulmala − *Aerosol and Haze Laboratory, Beijing Advanced Innovation Center for Soft Matter Science and Engineering, Beijing University of Chemical Technology, Beijing 100089, China; Institute for Atmospheric and Earth System Research/Physics, Faculty of Science, University of Helsinki, Helsinki 00560, Finland; Joint International Research Laboratory of Atmospheric and Earth System Sciences (JirLATEST), Nanjing University, Nanjing 210023, China;* Email: markku.kulmala@helsinki.fi

Hong He − *State Key Joint Laboratory of Environment Simulation and Pollution Control, Research Center for Eco-Environmental Sciences and Center for Excellence in Regional Atmospheric Environment, Institute of Urban Environment, Chinese Academy of Sciences, Beijing 100085, China;* Email: honghe@rcees.ac.cn

Authors

Lei Yao − *Aerosol and Haze Laboratory, Beijing Advanced Innovation Center for Soft Matter Science and Engineering, Beijing University of Chemical Technology, Beijing 100089, China; Institute for Atmospheric and Earth System Research/Physics, Faculty of Science, University of Helsinki, Helsinki 00560, Finland;* orcid.org/0000-0002-2680-1629

Xiaolong Fan − *Aerosol and Haze Laboratory, Beijing Advanced Innovation Center for Soft Matter Science and Engineering, Beijing University of Chemical Technology, Beijing 100089, China*

Chao Yan − *Institute for Atmospheric and Earth System Research/Physics, Faculty of Science, University of Helsinki, Helsinki 00560, Finland*

Theo Kurtén − *Department of Chemistry, University of Helsinki, Helsinki 00014, Finland;* orcid.org/0000-0002-6416-4931

Kaspar R. Daellenbach − *Institute for Atmospheric and Earth System Research/Physics, Faculty of Science, University of Helsinki, Helsinki 00560, Finland*

Chang Li − *Aerosol and Haze Laboratory, Beijing Advanced Innovation Center for Soft Matter Science and Engineering, Beijing University of Chemical Technology, Beijing 100089, China*

Yonghong Wang − *Institute for Atmospheric and Earth System Research/Physics, Faculty of Science, University of Helsinki, Helsinki 00560, Finland*

Yishuo Guo − *Aerosol and Haze Laboratory, Beijing Advanced Innovation Center for Soft Matter Science and Engineering, Beijing University of Chemical Technology, Beijing 100089, China*

Lubna Dada − *Institute for Atmospheric and Earth System Research/Physics, Faculty of Science, University of Helsinki, Helsinki 00560, Finland*

Matti P. Rissanen − *Aerosol Physics Laboratory, Physics Unit, Tampere University, Tampere 33100, Finland;* orcid.org/0000-0003-0463-8098

Jing Cai − *Institute for Atmospheric and Earth System Research/Physics, Faculty of Science, University of Helsinki, Helsinki 00560, Finland*

Yee Jun Tham − *Institute for Atmospheric and Earth System Research/Physics, Faculty of Science, University of Helsinki, Helsinki 00560, Finland*

Qiaozhi Zha − *Institute for Atmospheric and Earth System Research/Physics, Faculty of Science, University of Helsinki, Helsinki 00560, Finland*

Shaojun Zhang − *State Key Joint Laboratory of Environment Simulation and Pollution Control, State Environmental Protection Key Laboratory of Sources and Control of Air Pollution Complex, School of Environment, Tsinghua University, Beijing 100084, China;* orcid.org/0000-0002-2176-6174

Wei Du − *Institute for Atmospheric and Earth System Research/Physics, Faculty of Science, University of Helsinki, Helsinki 00560, Finland*

Miao Yu − *Institute of Urban Meteorology, China Meteorological Administration, Beijing 100081, China*

Feixue Zheng − *Aerosol and Haze Laboratory, Beijing Advanced Innovation Center for Soft Matter Science and Engineering, Beijing University of Chemical Technology, Beijing 100089, China*

Ying Zhou − *Aerosol and Haze Laboratory, Beijing Advanced Innovation Center for Soft Matter Science and Engineering, Beijing University of Chemical Technology, Beijing 100089, China*

Jenni Kontkanen − *Institute for Atmospheric and Earth System Research/Physics, Faculty of Science, University of Helsinki, Helsinki 00560, Finland*

Tommy Chan − *Institute for Atmospheric and Earth System Research/Physics, Faculty of Science, University of Helsinki, Helsinki 00560, Finland*

Jiali Shen − *Institute for Atmospheric and Earth System Research/Physics, Faculty of Science, University of Helsinki, Helsinki 00560, Finland*

Joni T. Kujansuu − *Aerosol and Haze Laboratory, Beijing Advanced Innovation Center for Soft Matter Science and Engineering, Beijing University of Chemical Technology, Beijing 100089, China; Institute for Atmospheric and Earth System Research/Physics, Faculty of Science, University of Helsinki, Helsinki 00560, Finland*

Juha Kangasluoma − *Aerosol and Haze Laboratory, Beijing Advanced Innovation Center for Soft Matter Science and Engineering, Beijing University of Chemical Technology, Beijing 100089, China; Institute for Atmospheric and Earth System*

https://dx.doi.org/10.1021/acs.estlett.0c00615
Environ. Sci. Technol. Lett. 2020, 7, 809−818

Research/Physics, Faculty of Science, University of Helsinki, Helsinki 00560, Finland; orcid.org/0000-0002-1639-1187

Jingkun Jiang − *State Key Joint Laboratory of Environment Simulation and Pollution Control, State Environmental Protection Key Laboratory of Sources and Control of Air Pollution Complex, School of Environment, Tsinghua University, Beijing 100084, China*

Lin Wang − *Shanghai Key Laboratory of Atmospheric Particle Pollution and Prevention (LAP3), Department of Environmental Science & Engineering, Fudan University, Shanghai 200438, China;* orcid.org/0000-0002-4905-3432

Douglas R. Worsnop − *Aerodyne Research Inc., Billerica, Massachusetts 01821, United States*

Tuukka Petäjä − *Institute for Atmospheric and Earth System Research/Physics, Faculty of Science, University of Helsinki, Helsinki 00560, Finland*

Veli-Matti Kerminen − *Institute for Atmospheric and Earth System Research/Physics, Faculty of Science, University of Helsinki, Helsinki 00560, Finland*

Yongchun Liu − *Aerosol and Haze Laboratory, Beijing Advanced Innovation Center for Soft Matter Science and Engineering, Beijing University of Chemical Technology, Beijing 100089, China;* orcid.org/0000-0002-9055-970X

Biwu Chu − *Institute for Atmospheric and Earth System Research/Physics, Faculty of Science, University of Helsinki, Helsinki 00560, Finland; State Key Joint Laboratory of Environment Simulation and Pollution Control, Research Center for Eco-Environmental Sciences and Center for Excellence in Regional Atmospheric Environment, Institute of Urban Environment, Chinese Academy of Sciences, Beijing 100085, China;* orcid.org/0000-0002-7548-5669

Complete contact information is available at: https://pubs.acs.org/10.1021/acs.estlett.0c00615

Author Contributions

L.Y. and X.F. contributed equally to this work. L.Y. and F.B. designed the research and analyzed the data. L.Y., C.Y., Y.G., C.L., X.F., Y.Z., K.R.D., F.Z., Y.W., and T.C. performed the measurements for this study. T.K. provided quantum calculation results. L.Y., X.F., B.C., F.B., T.P., M.P.R., L.W., Y.L., J.J., D.R.W., V.-M.K., T.K., and M.K. interpreted the results and revised the manuscript. M.K., F.B., and H.H. supported and supervised this research. L.Y. wrote the manuscript with contributions from all co-authors.

Notes

The authors declare no competing financial interest.

■ ACKNOWLEDGMENTS

The work is supported by Academy of Finland (Center of Excellence in Atmospheric Sciences, project no. 307331, and PROFI3 funding, 311932), the European Research Council via ATM-GTP (742206) and via CHAPAs (850614) and the EMME-CARE project which has received funding from the European Union's Horizon 2020 Research and Innovation Programme, under Grant Agreement No. 856612.

■ REFERENCES

(1) Larssen, T.; Lydersen, E.; Tang, D. G.; He, Y.; Gao, J. X.; Liu, H. Y.; Duan, L.; Seip, H. M.; Vogt, R. D.; Mulder, J.; Shao, M.; Wang, Y. H.; Shang, H.; Zhang, X. S.; Solberg, S.; Aas, W.; Okland, T.; Eilertsen, O.; Angell, V.; Li, Q. R.; Zhao, D. W.; Xiang, R. J.; Xiao, J. S.; Luo, J. H. Acid rain in China. *Environ. Sci. Technol.* **2006**, *40* (2), 418−425.

(2) Sipilä, M.; Berndt, T.; Petäjä, T.; Brus, D.; Vanhanen, J.; Stratmann, F.; Patokoski, J.; Mauldin, R. L.; Hyvarinen, A. P.; Lihavainen, H.; Kulmala, M. The Role of Sulfuric Acid in Atmospheric Nucleation. *Science* **2010**, *327* (5970), 1243−1246.

(3) Kulmala, M.; Kontkanen, J.; Junninen, H.; Lehtipalo, K.; Manninen, H. E.; Nieminen, T.; Petäjä, T.; Sipilä, M.; Schobesberger, S.; Rantala, P.; Franchin, A.; Jokinen, T.; Jarvinen, E.; Aijala, M.; Kangasluoma, J.; Hakala, J.; Aalto, P. P.; Paasonen, P.; Mikkila, J.; Vanhanen, J.; Aalto, J.; Hakola, H.; Makkonen, U.; Ruuskanen, T.; Mauldin, R. L.; Duplissy, J.; Vehkamaki, H.; Back, J.; Kortelainen, A.; Riipinen, I.; Kurtén, T.; Johnston, M. V.; Smith, J. N.; Ehn, M.; Mentel, T. F.; Lehtinen, K. E.; Laaksonen, A.; Kerminen, V. M.; Worsnop, D. R. Direct observations of atmospheric aerosol nucleation. *Science* **2013**, *339* (6122), 943−6.

(4) Bianchi, F.; Tröstl, J.; Junninen, H.; Frege, C.; Henne, S.; Hoyle, C. R.; Molteni, U.; Herrmann, E.; Adamov, A.; Bukowiecki, N.; Chen, X.; Duplissy, J.; Gysel, M.; Hutterli, M.; Kangasluoma, J.; Kontkanen, J.; Kurten, A.; Manninen, H. E.; Munch, S.; Perakyla, O.; Petäjä, T.; Rondo, L.; Williamson, C.; Weingartner, E.; Curtius, J.; Worsnop, D. R.; Kulmala, M.; Dommen, J.; Baltensperger, U. New particle formation in the free troposphere: A question of chemistry and timing. *Science* **2016**, *352* (6289), 1109−1112.

(5) Yao, L.; Garmash, O.; Bianchi, F.; Zheng, J.; Yan, C.; Kontkanen, J.; Junninen, H.; Mazon, S. B.; Ehn, M.; Paasonen, P.; Sipilä, M.; Wang, M.; Wang, X.; Xiao, S.; Chen, H.; Lu, Y.; Zhang, B.; Wang, D.; Fu, Q.; Geng, F.; Li, L.; Wang, H.; Qiao, L.; Yang, X.; Chen, J.; Kerminen, V. M.; Petäjä, T.; Worsnop, D. R.; Kulmala, M.; Wang, L. Atmospheric new particle formation from sulfuric acid and amines in a Chinese megacity. *Science* **2018**, *361* (6399), 278−281.

(6) Chu, B. W.; Kerminen, V. M.; Bianchi, F.; Yan, C.; Petäjä, T.; Kulmala, M. Atmospheric new particle formation in China. *Atmos. Chem. Phys.* **2019**, *19* (1), 115−138.

(7) Chen, H.; Wang, M.; Yao, L.; Chen, J.; Wang, L. Uptake of Gaseous Alkylamides by Suspended Sulfuric Acid Particles: Formation of Ammonium/Aminium Salts. *Environ. Sci. Technol.* **2017**, *51* (20), 11710−11717.

(8) Kerminen, V. M.; Chen, X. M.; Vakkari, V.; Petäjä, T.; Kulmala, M.; Bianchi, F. Atmospheric new particle formation and growth: review of field observations. *Environ. Res. Lett.* **2018**, *13* (10), 103003.

(9) Mauldin, R. L.; Berndt, T.; Sipilä, M.; Paasonen, P.; Petäjä, T.; Kim, S.; Kurtén, T.; Stratmann, F.; Kerminen, V. M.; Kulmala, M. A new atmospherically relevant oxidant of sulphur dioxide. *Nature* **2012**, *488* (7410), 193−196.

(10) Welz, O.; Savee, J. D.; Osborn, D. L.; Vasu, S. S.; Percival, C. J.; Shallcross, D. E.; Taatjes, C. A. Direct Kinetic Measurements of Criegee Intermediate (CH_2OO) Formed by Reaction of CH_2I with O_2. *Science* **2012**, *335* (6065), 204−207.

(11) He, G. Z.; He, H. DFT studies on the heterogeneous oxidation of SO_2 by oxygen functional groups on graphene. *Phys. Chem. Chem. Phys.* **2016**, *18* (46), 31691−31697.

(12) He, G. Z.; Ma, J. Z.; He, H. Role of Carbonaceous Aerosols in Catalyzing Sulfate Formation. *ACS Catal.* **2018**, *8* (5), 3825−3832.

(13) Lizzio, A. A.; DeBarr, J. A. Mechanism of SO_2 removal by carbon. *Energy Fuels* **1997**, *11* (2), 284−291.

(14) Han, C.; Liu, Y. C.; Ma, J. Z.; He, H. Key role of organic carbon in the sunlight-enhanced atmospheric aging of soot by O_2. *Proc. Natl. Acad. Sci. U. S. A.* **2012**, *109* (52), 21250−21255.

(15) He, G.; He, H. Water Promotes the Oxidation of SO_2 by O_2 over Carbonaceous Aerosols. *Environ. Sci. Technol.* **2020**, *54* (12), 7070−7077.

(16) Novakov, T.; Chang, S. G.; Harker, A. B. Sulfates as Pollution Particulates - Catalytic Formation on Carbon (soot) Particles. *Science* **1974**, *186* (4160), 259−261.

(17) Zhao, Y.; Liu, Y. C.; Ma, J. Z.; Ma, Q. X.; He, H. Heterogeneous reaction of SO_2 with soot: The roles of relative

humidity and surface composition of soot in surface sulfate formation. *Atmos. Environ.* **2017**, *152*, 465−476.
(18) He, X.; Pang, S. F.; Ma, J. B.; Zhang, Y. H. Influence of relative humidity on heterogeneous reactions of O_3 and O_3/SO_2 with soot particles: Potential for environmental and health effects. *Atmos. Environ.* **2017**, *165*, 198−206.
(19) Zhang, F.; Wang, Y.; Peng, J.; Chen, L.; Sun, Y.; Duan, L.; Ge, X.; Li, Y.; Zhao, J.; Liu, C.; Zhang, X.; Zhang, G.; Pan, Y.; Wang, Y.; Zhang, A. L.; Ji, Y.; Wang, G.; Hu, M.; Molina, M. J.; Zhang, R. An unexpected catalyst dominates formation and radiative forcing of regional haze. *Proc. Natl. Acad. Sci. U. S. A.* **2020**, *117* (8), 3960−3966.
(20) Shen, J. L.; Zheng, C. H.; Xu, L. J.; Zhang, Y.; Zhang, Y. X.; Liu, S. J.; Gao, X. Atmospheric emission inventory of SO_3 from coal-fired power plants in China in the period 2009−2014. *Atmos. Environ.* **2019**, *197*, 14−21.
(21) Yang, Z.; Ji, P.; Li, Q.; Jiang, Y.; Zheng, C.; Wang, Y.; Gao, X.; Lin, R. Comprehensive understanding of SO_3 effects on synergies among air pollution control devices in ultra-low emission power plants burning high-sulfur coal. *J. Cleaner Prod.* **2019**, *239*, 118096.
(22) Roy, B.; Chen, L. G.; Bhattacharya, S. Nitrogen Oxides, Sulfur Trioxide, and Mercury Emissions during Oxyfuel Fluidized Bed Combustion of Victorian Brown Coal. *Environ. Sci. Technol.* **2014**, *48* (24), 14844−14850.
(23) Morokuma, K.; Muguruma, C. Ab-Initio Molecular-Orbital Study of the Mechanism of the Gas-Phase Reaction SO_3+H_2O - Importance of the 2nd Water Molecule. *J. Am. Chem. Soc.* **1994**, *116* (22), 10316−10317.
(24) Kolb, C. E.; Jayne, J. T.; Worsnop, D. R.; Molina, M. J.; Meads, R. F.; Viggiano, A. A. Gas-Phase Reaction of Sulfur-Trioxide with Water-Vapor. *J. Am. Chem. Soc.* **1994**, *116* (22), 10314−10315.
(25) Li, H.; Zhong, J.; Vehkamaki, H.; Kurten, T.; Wang, W. G.; Ge, M. F.; Zhang, S. W.; Li, Z. S.; Zhang, X. H.; Francisco, J. S.; Zeng, X. C. Self-Catalytic Reaction of SO_3 and NH_3 To Produce Sulfamic Acid and Its Implication to Atmospheric Particle Formation. *J. Am. Chem. Soc.* **2018**, *140* (35), 11020−11028.
(26) Sarkar, S.; Oram, B. K.; Bandyopadhyay, B. Influence of Ammonia and Water on the Fate of Sulfur Trioxide in the Troposphere: Theoretical Investigation of Sulfamic Acid and Sulfuric Acid Formation Pathways. *J. Phys. Chem. A* **2019**, *123* (14), 3131−3141.
(27) Lv, G. C.; Sun, X. M.; Zhang, C. X.; Li, M. Understanding the catalytic role of oxalic acid in SO_3 hydration to form H_2SO_4 in the atmosphere. *Atmos. Chem. Phys.* **2019**, *19* (5), 2833−2844.
(28) Bandyopadhyay, B.; Kumar, P.; Biswas, P. Ammonia Catalyzed Formation of Sulfuric Acid in Troposphere: The Curious Case of a Base Promoting Acid Rain. *J. Phys. Chem. A* **2017**, *121* (16), 3101−3108.
(29) Long, B.; Chang, C. R.; Long, Z. W.; Wang, Y. B.; Tan, X. F.; Zhang, W. J. Nitric acid catalyzed hydrolysis of SO_3 in the formation of sulfuric acid: A theoretical study. *Chem. Phys. Lett.* **2013**, *581*, 26−29.
(30) Fleig, D.; Vainio, E.; Andersson, K.; Brink, A.; Johnsson, F.; Hupa, M. Evaluation of SO3Measurement Techniques in Air and Oxy-Fuel Combustion. *Energy Fuels* **2012**, *26* (9), 5537−5549.
(31) Lovejoy, E. R.; Hanson, D. R.; Huey, L. G. Kinetics and products of the gas-phase reaction of SO_3 with water. *J. Phys. Chem.* **1996**, *100* (51), 19911−19916.
(32) Arnold, S. T.; Morris, R. A.; Viggiano, A. A.; Jayne, J. T. Ion Chemistry Relevant for Chemical-Ionization Detection of SO_3. *J. Geophys. Res.* **1995**, *100* (D7), 14141−14146.
(33) Jayne, J. T.; Poschl, U.; Chen, Y. M.; Dai, D.; Molina, L. T.; Worsnop, D. R.; Kolb, C. E.; Molina, M. J. Pressure and temperature dependence of the gas-phase reaction of SO_3 with H_2O and the heterogeneous reaction of SO_3 with H_2O/H_2SO_4 surfaces. *J. Phys. Chem. A* **1997**, *101* (51), 10000−10011.
(34) Sorokin, A.; Katragkou, E.; Arnold, F.; Busen, R.; Schumann, U. Gaseous SO_3 and H_2SO_4 in the exhaust of an aircraft gas turbine engine: measurements by CIMS and implications for fuel sulfur conversion to sulfur (VI) and conversion of SO_3 to H_2SO_4. *Atmos. Environ.* **2004**, *38* (3), 449−456.
(35) Berndt, T.; Scholz, W.; Mentler, B.; Fischer, L.; Hoffmann, E. H.; Tilgner, A.; Hyttinen, N.; Prisle, N. L.; Hansel, A.; Herrmann, H. Fast Peroxy Radical Isomerization and OH Recycling in the Reaction of OH Radicals with Dimethyl Sulfide. *J. Phys. Chem. Lett.* **2019**, *10* (21), 6478−6483.
(36) Jokinen, T.; Sipilä, M.; Junninen, H.; Ehn, M.; Lönn, G.; Hakala, J.; Petäjä, T.; Mauldin, R. L.; Kulmala, M.; Worsnop, D. R. Atmospheric sulphuric acid and neutral cluster measurements using CI-APi-TOF. *Atmos. Chem. Phys.* **2012**, *12* (9), 4117−4125.
(37) Kürten, A.; Rondo, L.; Ehrhart, S.; Curtius, J. Calibration of a chemical ionization mass spectrometer for the measurement of gaseous sulfuric acid. *J. Phys. Chem. A* **2012**, *116* (24), 6375−86.
(38) Mohler, O.; Reiner, T.; Arnold, F. The Formation of SO_5^- by Gas-Phase Ion−Molecule Reactions. *J. Chem. Phys.* **1992**, *97* (11), 8233−8239.
(39) Anglada, J. M.; Hoffman, G. J.; Slipchenko, L. V.; Costa, M. M.; Ruiz-Lopez, M. F.; Francisco, J. S. Atmospheric Significance of Water Clusters and Ozone-Water Complexes. *J. Phys. Chem. A* **2013**, *117* (40), 10381−10396.
(40) Larson, L. J.; Kuno, M.; Tao, F. M. Hydrolysis of sulfur trioxide to form sulfuric acid in small water clusters. *J. Chem. Phys.* **2000**, *112* (20), 8830−8838.
(41) Yang, D. Y.; Zhang, S. J.; Niu, T. L.; Wang, Y. J.; Xu, H. L.; Zhang, K. M.; Wu, Y. High-resolution mapping of vehicle emissions of atmospheric pollutants based on large-scale, real-world traffic datasets. *Atmos. Chem. Phys.* **2019**, *19* (13), 8831−8843.
(42) Xu, W. Y.; Zhao, C. S.; Ran, L.; Lin, W. L.; Yan, P.; Xu, X. B. SO_2 noontime-peak phenomenon in the North China Plain. *Atmos. Chem. Phys.* **2014**, *14* (15), 7757−7768.
(43) Liu, J.; Mauzerall, D. L.; Chen, Q.; Zhang, Q.; Song, Y.; Peng, W.; Klimont, Z.; Qiu, X. H.; Zhang, S. Q.; Hu, M.; Lin, W. L.; Smith, K. R.; Zhu, T. Air pollutant emissions from Chinese households: A major and underappreciated ambient pollution source. *Proc. Natl. Acad. Sci. U. S. A.* **2016**, *113* (28), 7756−7761.
(44) Li, R.; Fu, H. B.; Cui, L. L.; Li, J. L.; Wu, Y.; Meng, Y.; Wang, Y. T.; Chen, J. M. The spatiotemporal variation and key factors of SO_2 in 336 cities across China. *J. Cleaner Prod.* **2019**, *210*, 602−611.
(45) Huang, Q.; Cheng, S. Y.; Perozzi, R. E.; Perozzi, E. F. Use of a MM5-CAMx-PSAT Modeling System to Study SO_2 Source Apportionment in the Beijing Metropolitan Region. *Environ. Model. Assess.* **2012**, *17* (5), 527−538.
(46) Kampa, M.; Castanas, E. Human health effects of air pollution. *Environ. Pollut.* **2008**, *151* (2), 362−367.
(47) Zhong, Q. R.; Shen, H. Z.; Yun, X.; Chen, Y. L.; Ren, Y. A.; Xu, H. R.; Shen, G. F.; Ma, J. M.; Tao, S. Effects of International Fuel Trade on Global Sulfur Dioxide Emissions. *Environ. Sci. Technol. Lett.* **2019**, *6* (12), 727−731.
(48) Klimont, Z.; Smith, S. J.; Cofala, J. The last decade of global anthropogenic sulfur dioxide: 2000−2011 emissions. *Environ. Res. Lett.* **2013**, *8* (1), 014003.
(49) Su, S. S.; Li, B. G.; Cui, S. Y.; Tao, S. Sulfur Dioxide Emissions from Combustion in China: From 1990 to 2007. *Environ. Sci. Technol.* **2011**, *45* (19), 8403−8410.
(50) Zheng, H. T.; Cai, S. Y.; Wang, S. X.; Zhao, B.; Chang, X.; Hao, J. M. Development of a unit-based industrial emission inventory in the Beijing-Tianjin-Hebei region and resulting improvement in air quality modeling. *Atmos. Chem. Phys.* **2019**, *19* (6), 3447−3462.
(51) Rohrer, F.; Lu, K. D.; Hofzumahaus, A.; Bohn, B.; Brauers, T.; Chang, C. C.; Fuchs, H.; Haseler, R.; Holland, F.; Hu, M.; Kita, K.; Kondo, Y.; Li, X.; Lou, S. R.; Oebel, A.; Shao, M.; Zeng, L. M.; Zhu, T.; Zhang, Y. H.; Wahner, A. Maximum efficiency in the hydroxyl-radical-based self-cleansing of the troposphere. *Nat. Geosci.* **2014**, *7* (8), 559−563.

https://dx.doi.org/10.1021/acs.estlett.0c00615
Environ. Sci. Technol. Lett. 2020, 7, 809−818

(52) Lu, K. D.; Rohrer, F.; Holland, F.; Fuchs, H.; Brauers, T.; Oebel, A.; Dlugi, R.; Hu, M.; Li, X.; Lou, S. R.; Shao, M.; Zhu, T.; Wahner, A.; Zhang, Y. H.; Hofzumahaus, A. Nighttime observation and chemistry of HOx in the Pearl River Delta and Beijing in summer 2006. *Atmos. Chem. Phys.* **2014**, *14* (10), 4979−4999.
(53) Tan, Z.; Fuchs, H.; Lu, K.; Hofzumahaus, A.; Bohn, B.; Broch, S.; Dong, H.; Gomm, S.; Häseler, R.; He, L.; Holland, F.; Li, X.; Liu, Y.; Lu, S.; Rohrer, F.; Shao, M.; Wang, B.; Wang, M.; Wu, Y.; Zeng, L.; Zhang, Y.; Wahner, A.; Zhang, Y. Radical chemistry at a rural site (Wangdu) in the North China Plain: observation and model calculations of OH, HO_2 and RO_2 radicals. *Atmos. Chem. Phys.* **2017**, *17* (1), 663−690.
(54) Tan, Z. F.; Rohrer, F.; Lu, K. D.; Ma, X. F.; Bohn, B.; Broch, S.; Dong, H. B.; Fuchs, H.; Gkatzelis, G. I.; Hofzumahaus, A.; Holland, F.; Li, X.; Liu, Y.; Liu, Y. H.; Novelli, A.; Shao, M.; Wang, H. C.; Wu, Y. S.; Zeng, L. M.; Hu, M.; Kiendler-Scharr, A.; Wahner, A.; Zhang, Y. H. Wintertime photochemistry in Beijing: observations of ROx radical concentrations in the North China Plain during the BEST-ONE campaign. *Atmos. Chem. Phys.* **2018**, *18* (16), 12391−12411.
(55) Lu, K.; Fuchs, H.; Hofzumahaus, A.; Tan, Z.; Wang, H.; Zhang, L.; Schmitt, S. H.; Rohrer, F.; Bohn, B.; Broch, S.; Dong, H.; Gkatzelis, G. I.; Hohaus, T.; Holland, F.; Li, X.; Liu, Y.; Liu, Y.; Ma, X.; Novelli, A.; Schlag, P.; Shao, M.; Wu, Y.; Wu, Z.; Zeng, L.; Hu, M.; Kiendler-Scharr, A.; Wahner, A.; Zhang, Y. Fast Photochemistry in Wintertime Haze: Consequences for Pollution Mitigation Strategies. *Environ. Sci. Technol.* **2019**, *53* (18), 10676−10684.
(56) Srivastava, R. K.; Miller, C. A.; Erickson, C.; Jambhekar, R. Emissions of sulfur trioxide from coal-fired power plants. *J. Air Waste Manage. Assoc.* **2004**, *54* (6), 750−762.
(57) Yang, Z. D.; Zheng, C. H.; Zhang, X. F.; Zhou, H.; Silva, A. A.; Liu, C. Y.; Snyder, B.; Wang, Y.; Gao, X. Challenge of SO_3 removal by wet electrostatic precipitator under simulated flue gas with high SO_3 concentration. *Fuel* **2018**, *217*, 597−604.
(58) Guo, Y.; Yan, C.; Li, C.; Feng, Z.; Zhou, Y.; Lin, Z.; Dada, L.; Stolzenburg, D.; Yin, R.; Kontkanen, J.; Daellenbach, K. R.; Kangasluoma, J.; Yao, L.; Chu, B.; Wang, Y.; Cai, R.; Bianchi, F.; Liu, Y.; Kulmala, M. *Atmos. Chem. Phys. Discuss.* **2020**, DOI: 10.5194/acp-2019-1111.
(59) Yao, L.; Wang, M.-Y.; Wang, X.-K.; Liu, Y.-J.; Chen, H.-F.; Zheng, J.; Nie, W.; Ding, A.-J.; Geng, F.-H.; Wang, D.-F.; Chen, J.-M.; Worsnop, D. R.; Wang, L. Detection of atmospheric gaseous amines and amides by a high-resolution time-of-flight chemical ionization mass spectrometer with protonated ethanol reagent ions. *Atmos. Chem. Phys.* **2016**, *16* (22), 14527−14543.
(60) Liu, L.; Zhong, J.; Vehkamaki, H.; Kurten, T.; Du, L.; Zhang, X.; Francisco, J. S.; Zeng, X. C. Unexpected quenching effect on new particle formation from the atmospheric reaction of methanol with SO_3. *Proc. Natl. Acad. Sci. U. S. A.* **2019**, *116* (50), 24966−24971.
(61) Olin, M.; Kuuluvainen, H.; Aurela, M.; Kalliokoski, J.; Kuittinen, N.; Isotalo, M.; Timonen, H. J.; Niemi, J. V.; Rönkkö, T.; Dal Maso, M. Traffic-originated nanocluster emission exceeds H_2SO_4-driven photochemical new particle formation in an urban area. *Atmos. Chem. Phys.* **2020**, *20* (1), 1−13.
(62) Ronkko, T.; Kuuluvainen, H.; Karjalainen, P.; Keskinen, J.; Hillamo, R.; Niemi, J. V.; Pirjola, L.; Timonen, H. J.; Saarikoski, S.; Saukko, E.; Jarvinen, A.; Silvennoinen, H.; Rostedt, A.; Olin, M.; Yli-Ojanpera, J.; Nousiainen, P.; Kousa, A.; Dal Maso, M. Traffic is a major source of atmospheric nanocluster aerosol. *Proc. Natl. Acad. Sci. U. S. A.* **2017**, *114* (29), 7549−7554.

https://dx.doi.org/10.1021/acs.estlett.0c00615
Environ. Sci. Technol. Lett. 2020, 7, 809−818